ADVANCED MATERIALS

Supporting Information

for *Adv. Mater.*, DOI 10.1002/adma.202210941

Multi-Resonant Mie Resonator Arrays for Broadband Light Trapping in Ultrathin c-Si Solar Cells

*Nayeun Lee, Muyu Xue, Jiho Hong, Jorik van de Groep and Mark Luitzen Brongersma**

Supplementary Information

Multi-resonant Mie resonator arrays for broadband light trapping in ultrathin c-Si solar cells

Nayeun Lee[1], Muyu Xue[1], Jiho Hong[1], Jorik van de Groep[1], Mark L. Brongersma[1]*

[1] Geballe Laboratory for Advanced Materials, Stanford University, Stanford, California, USA

[*] Corresponding author. Email: brongersma@stanford.edu

[†] Current address: Van der Waals–Zeeman Institute for Experimental Physics, Institute of Physics, University of Amsterdam, Amsterdam, Netherlands.

This PDF file includes:

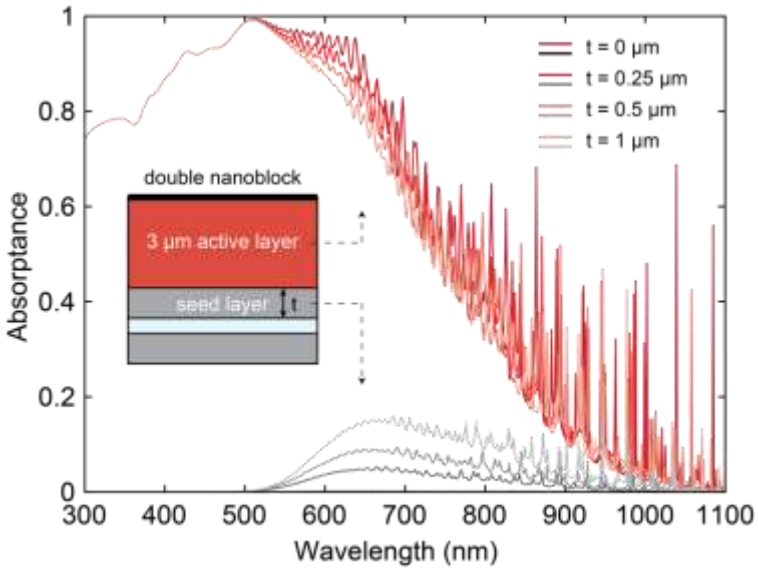

Supplementary Figure 1 | Simulated absorptance spectra of the ultrathin Si solar cells with different seed layer thickness. Depending on the seed layer thickness, absorptance spectra of a 3-μm-thick active layer (red) and corresponding seed layer (gray) are plotted. Solar cells with the double-nanoblock-array are assumed. Estimated J_{sc} from the absorptance spectra are 24.87, 24.22, 23.84, 23.28 mA/cm^2, for seed layer thickness of 0, 0.25, 0.5, 1 μm respectively.

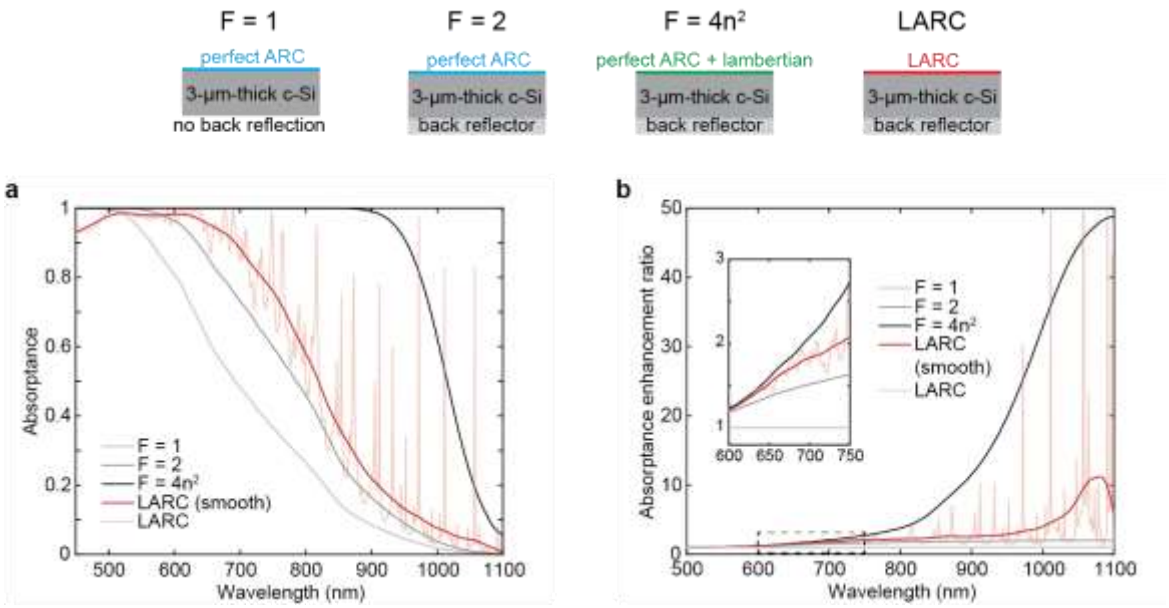

Supplementary Figure 2 | Simulated absorptance of 3-μm-thick c-Si solar cells with various light-trapping schemes. a) Simulated absorptance spectra. b) Simulated absorptance enhancement ratio of various light-trapping schemes to the single-pass absorption (optical path enhancement factor, F = 1). Inset: absorptance enhancement ratio spectra magnified in the 600 – 750 nm wavelength range. To study the effect of the LARC on light absorption, we compare these four ideal structures: a 3-μm-thick c-Si solar cell with a perfect ARC and no back reflector (single-pass absorption, F = 1), with a perfect ARC and a perfect back reflector (double-pass absorption, F = 2), with a perfect ARC and Lambertian scattering on top and a perfect back reflector (Yablonovitch limit, $F = 4n^2$), with a LARC and a perfect back reflector. An ultrathin cell using the nanostructured LARC presents a higher absorptance compared to the double-pass absorption over a wide spectral range in the solar spectrum, indicating the broadband light-trapping. Especially, a significant absorption enhancement is observed in the wavelength range of 500 – 800 nm where the light is efficiently redirected via Mie resonances. At the longer wavelengths, guided resonances supported by the Si slab also contribute to the absorption enhancement.

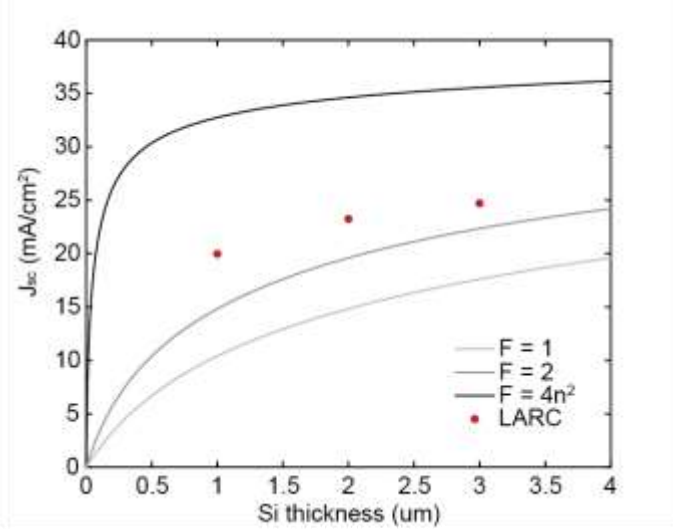

Supplementary Figure 3 | Calculated J_{sc} of c-Si solar cells with various light-trapping schemes depending on the cell thickness. Structures used for the calculation are illustrated in Supplementary Figure 2. A solar cell with the LARC and a back reflector achieves a larger J_{sc} compared to the double-pass absorption, which is expected from Supplementary Figure 2. Note that the proposed nanophotonic design for light trapping and antireflection generally applies regardless of the thickness of solar cells. This is possible by using the multi-resonant Mie-resonator array that effectively cancels out the reflection and redistributes the transmitted broadband sunlight at the topmost surface. In the design process, we do not utilize additional optical modes supported by the active layer. Therefore, it is possible to apply the proposed nanostructure for the solar cells with a wide range of thicknesses. Especially, the current LARC design offers much more effective light trapping for the thin c-Si layer for which the double optical pass is not enough to fully absorb sunlight. This well explains why the LARC achieves an increased J_{sc} compared to the double-pass absorption for ultrathin cells (< a few μm) where the light trapping plays a significant role. In this work, we are mainly targeting to create a nanophotonic design for ultrathin solar cells, on which micron-sized conventional random surface texturing is difficult to be applied. For a thicker c-Si layer, the design of a nanoblock-array can be re-optimized in order to efficiently redistribute light at longer wavelengths by red-shifting the Mie resonances.

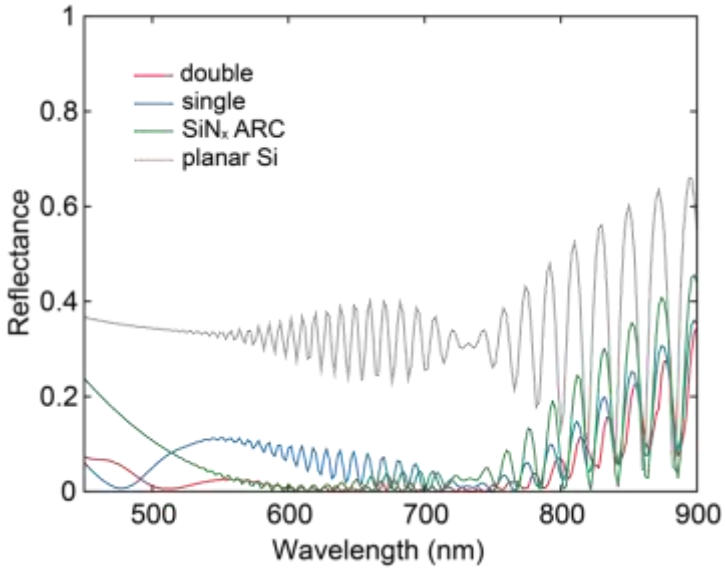

Supplementary Figure 4 | Simulated reflectance spectra of the ultrathin Si solar cells with different photon management schemes. In all designs, Si surfaces are conformally coated with the 25-nm-thick SiO_2 passivation layer.

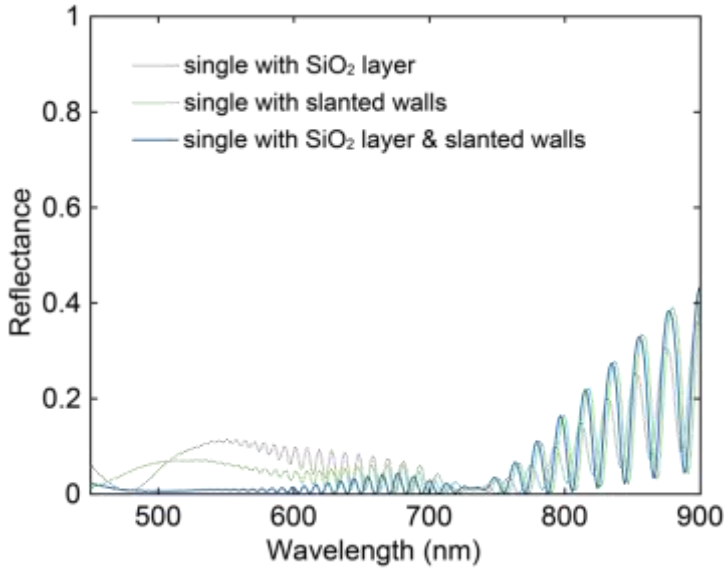

Supplementary Figure 5 | Spectral broadening due to the SiO_2 passivation layer and slanted walls of nanostructures. Reflectance spectra are simulated for the ultrathin c-Si solar cells with different designs of the single-nanoblock-arrays. The grey line is the reflectance spectrum of the single-nanoblock-array with the 25-nm-thick SiO_2 passivation layer assuming vertical side walls of the nanoblocks, which is the same design as in the Supplementary Figure 4. The green line is the reflectance spectrum of the single-nanoblock-array with the slanted walls and without the SiO_2 layer. The blue line is the reflectance spectrum of the single-nanoblock-array with both the SiO_2 layer and the slanted walls. Both the SiO_2 layer and the slanted walls of the nanoblocks give rise to spectral broadening, resulting in further suppression of the reflection. The geometric parameters of the slanted walls are extracted from the cross-sectional SEM image (inset to Figure 4a). For the simulations without the SiO_2 layer (green), the widths of the Si nanoblocks are increased by 25 nm, taking account of the size variation during the surface passivation process.

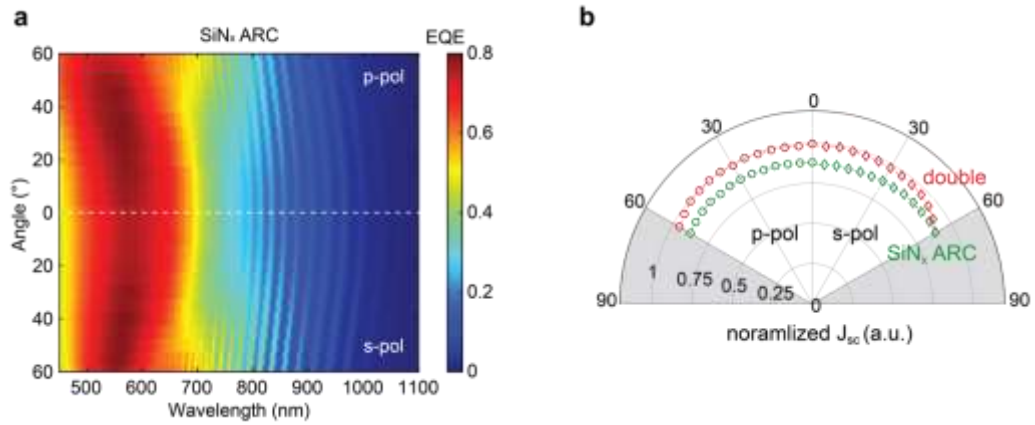

Supplementary Figure 6 | Additional information on angle-dependent characteristic of devices. a) Measured EQE spectra of a device with the SiN_x ARC as a function of incident angle. b) Polar plot of estimated J_{sc} from the measured EQE spectra as a function of the incident angle. J_{sc} are normalized to the value of the double-nanoblock-array at normal incidence.

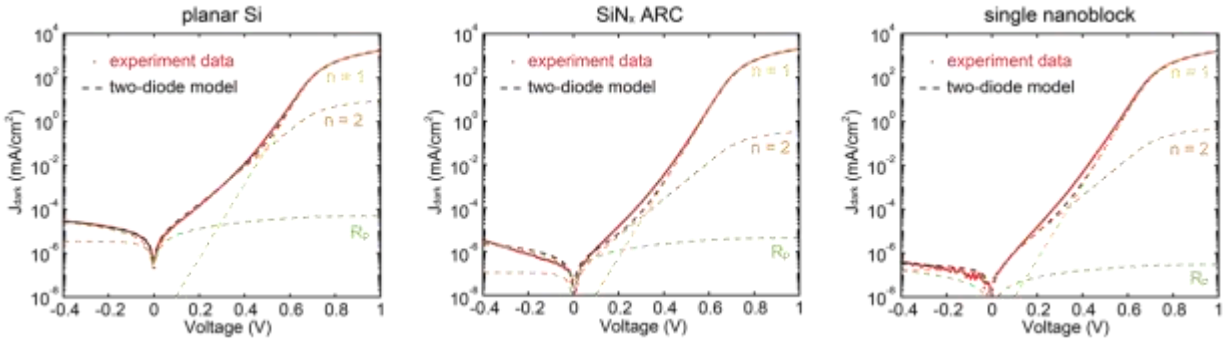

Supplementary Figure 7 | Measured dark J-V curves of the ultrathin Si solar cells with different photon management layers. Measurements with the planar Si, SiN_x ARC, and single-nanoblock-array correspond to left, middle and right panel, respectively. Experiment data (red dots) are fitted with a two-diode model (black dashed line). Each contribution from first diode current (n=1, yellow), second diode current (n=2, orange), and parallel resistance (R_p, green) is drawn together.

	nanopatterning	J_{01} (mA/cm^2)
double nanoblock	○	2.16×10^{-10}
single nanoblock	○	2.09×10^{-10}
SiN_x ARC	×	2.30×10^{-10}
planar Si	×	2.39×10^{-10}

Supplementary Table 1 | J_{01} values of devices with and without nanopatterning.

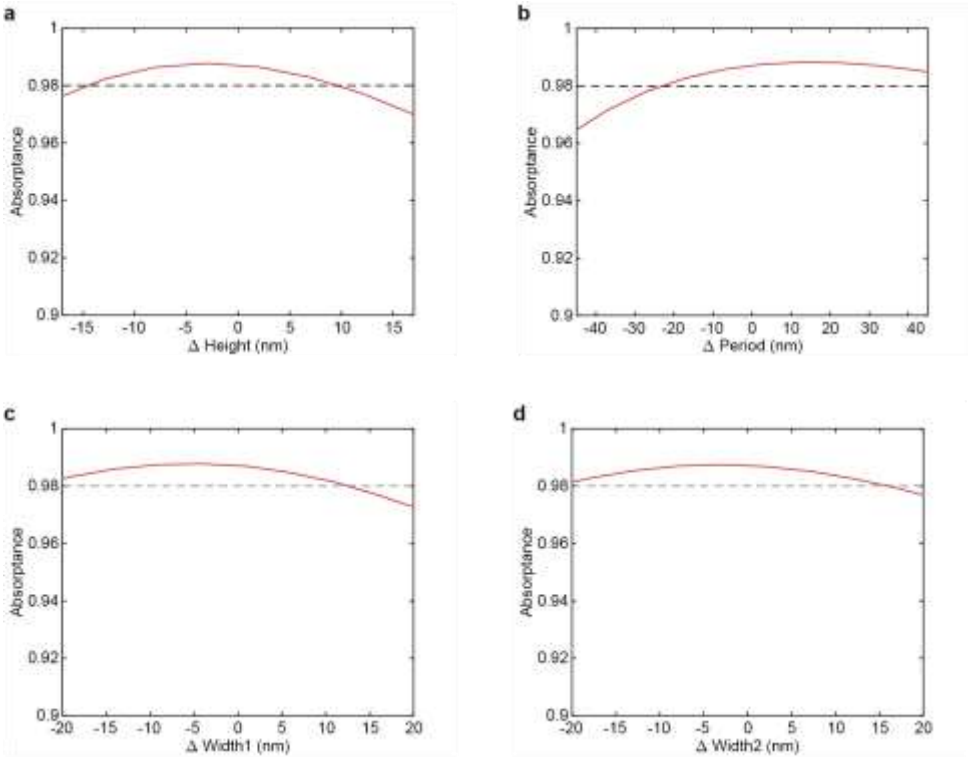

Supplementary Figure 8 | Simulated absorptance of a semi-infinite Si substrate with the double-nanoblock-array while changing individual structural parameters of the nanoblocks. The design has a high tolerance for the changes in the structural parameters which stems from the low-*Q* nature of the resonances supported by the nanoblock-array. As a reference, we show a line of 98% average absorptance, revealing the tolerance of the design to be more than 25 nm in all geometrical design parameters. The values for the height, period, width1 and width2 come from the fabricated double-nanoblock-array and the absorptance is averaged over the 450 – 900 nm spectral range.

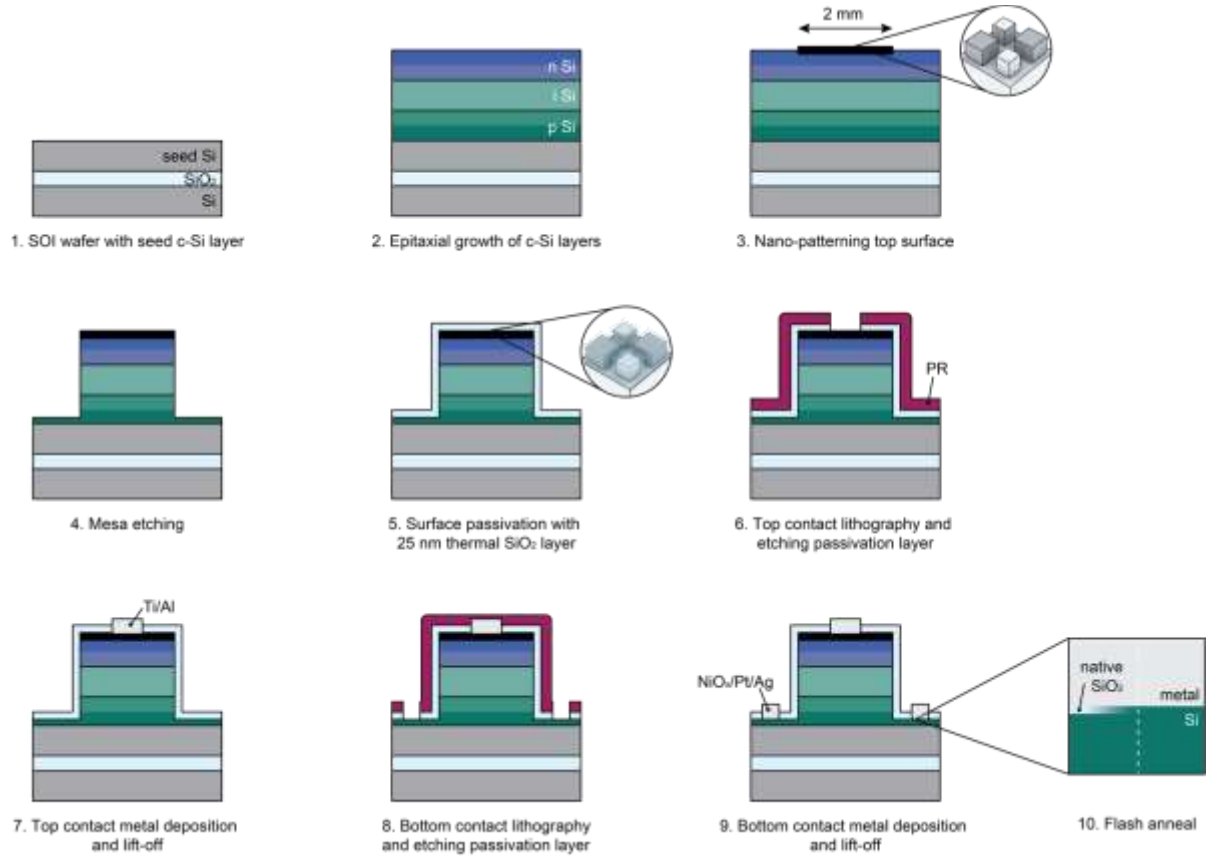

Supplementary Figure 9 | Schematics of the ultrathin c-Si solar cell fabrication process. Four types of devices are fabricated within the same wafer. For reference cells (planar Si and SiN_x ARC), step 3 is skipped. For reference cells with SiN_x ARC, SiN_x is deposited between step 5 and step 6.